

Impact Point Prediction of Small Ballistic Munitions with an Interacting Multiple Model Estimator

Steve Conover^a, J. Clayton Kerce^a, George Brown^a, Lisa Ehrman^a, and David Hardiman^b

^aGeorgia Tech Research Institute, Atlanta, GA 30332

^bAviation and Missile RDEC, AMSRD-AMR-SG-CT, Huntsville, AL

ABSTRACT

The interacting multiple model (IMM) estimator, which mixes and blends results of multiple filters according to their mode probabilities, is frequently used to track targets whose motion is not well-captured by a single model. This paper extends the use of an IMM estimator to computing impact point predictions (IPPs) of small ballistic munitions whose motion models change when they reach transonic and supersonic speeds. Three approaches for computing IPPs are compared. The first approach propagates only the track from the most likely mode until it impacts the ground. Since this approach neglects inputs from the other modes, it is not desirable if multiple modes have near-equal probabilities. The second approach for computing IPPs propagates tracks from each model contained in the IMM estimator to the ground independent of each other and combines the resulting state estimates and covariances on the ground via a weighted sum in which weights are the model probabilities. The final approach investigated here is designed to take advantage of the computational savings of the first without sacrificing input from any of the IMM's modes. It fuses the tracks from the models together and propagates the fused track to the ground. Note that the second and third approaches reduce to the first if one of the models has a mode probability of one. Results from all three approaches are compared in simulation.

Keywords: Interacting Multiple Model, Impact Point Prediction

1. INTRODUCTION

The interacting multiple model (IMM) estimator, which mixes and blends results of multiple filters according to their mode probabilities, is frequently used to track targets whose motion is not well-captured by a single model [1,2,3,4]. This paper examines the use of an IMM estimator in computing impact point predictions (IPPs) for small ballistic munitions whose motion models vary at subsonic, transonic, and supersonic speeds. Such munitions exhibit variable drag characteristics depending on the mach regime the projectile occupies, and the rate of change of drag with Mach number is generally largest in the transonic regime. The approach taken in this paper is to model projectile motion in the tracker with two types of dynamics, further assigning a high process noise and low process noise filter for each of these types of dynamics. The desire in breaking out these types of dynamic models is to capture well behaved drag characteristics in the supersonic and subsonic regimes, while allowing enough model uncertainty in the transonic regime to maintain a good track. The first dynamic model, the A-filter (acceleration-filter), assumes ideal point mass motion under the influence of gravity, drag, and a constant acceleration; the second filter considered here will be referred to as the B-filter (ballistic-filter), and includes only dynamic accelerations arising from gravity and drag along the velocity component of the projectile center of mass. The A-filter acceleration is included to model the cross range motion observed in spin stabilized projectiles, while the B-filter models a fin stabilized projectile.

Three approaches for computing IPP estimates are compared. The first approach propagates only the track from the most likely mode until it impacts the ground. Since this approach neglects inputs from the other modes, it may not be desirable if multiple modes have near-equal probabilities, since the average of two equally likely models can be better than either one independently. The second approach for computing IPPs propagates tracks from each model contained in the IMM estimator to the ground independent of each other and combines the resulting state estimates and covariances on the ground via a weighted sum in which weights are the model probabilities. The third approach is designed to take advantage of the computational savings of the first without sacrificing input from any of the IMM's modes. It fuses the tracks from the models together and propagates the fused track to the ground. Note that the second

and third approaches reduce to the first if one of the modes has a probability of one. Results from all three approaches are compared in a high-fidelity radar simulation.

2. MODEL DYNAMICS

Two types of target dynamics are considered for the IPP estimation. The simplest includes only gravity and a drag force that is collinear with the projectile velocity, representing forces of simple ballistic motion. We take the state vector of the system to be $x = x_p, x_v, x_{\Delta\beta}, x_{\beta_0}$, where x_p represents the target position, x_v the target velocity, $x_{\Delta\beta}$ a correction term to the ballistic coefficient, and x_{β_0} the first initial estimate of the ballistic coefficient as computed on filter startup. The last state, x_{β_0} , is static under both target dynamics and filter updates, and for that reason can be regarded as an auxiliary variable. The equations of motion for B-filter are given in terms of the state variables, the altitude variable air density, ρ , and the flat Earth gravitational acceleration g as follows:

$$\begin{aligned} \frac{d}{dt} \mathbf{x}_p &= \mathbf{x}_v & \mathbf{x}_p(t) \Big|_{t=0} &= \mathbf{x}_{p,0}, \\ \frac{d}{dt} \mathbf{x}_v &= \mathbf{g} - \frac{\rho}{2\mathbf{x}_{\beta_0}} |\mathbf{x}_v| \mathbf{x}_v + \frac{\rho}{2\mathbf{x}_{\beta_0}^2} |\mathbf{x}_v| \mathbf{x}_v \mathbf{x}_{\Delta\beta} & \mathbf{x}_v(t) \Big|_{t=0} &= \mathbf{x}_{v,0}, \\ \frac{d}{dt} \mathbf{x}_{\Delta\beta} &= 0 & \mathbf{x}_{\Delta\beta}(t) \Big|_{t=0} &= \mathbf{x}_{\Delta\beta,0}, \\ \frac{d}{dt} \mathbf{x}_{\beta_0} &= 0 & \mathbf{x}_{\beta_0}(t) \Big|_{t=0} &= \mathbf{x}_{\beta_0}. \end{aligned}$$

, with initial conditions

The dynamical equation for x_v merits some discussion, since it is the standard acceleration equation for velocity dependent drag written in terms of nonstandard variables x_{β_0} and $x_{\Delta\beta}$. This equation is more commonly represented in the form $\dot{\mathbf{v}} = \mathbf{g} - \gamma |\mathbf{v}| \mathbf{v}$, where v is the velocity and γ is the drag coefficient. As mentioned above, we have chosen to write the drag coefficient in terms of the altitude varying air density and the ballistic coefficient. Denoting the ballistic coefficient by β , we can write the drag coefficient

$$\gamma = \frac{\rho}{2\beta}.$$

This coefficient varies as a function of velocity, and usually exhibits the characteristics of the example drag coefficient function shown in Figure 1 [5], where it is shown as a function of the Mach number. The Mach number is the projectile speed divided by the speed of sound. The example curve demonstrates three generic regimes, subsonic, transonic, and supersonic. The subsonic regime is that velocity range in which pressure waves that develop due to the objects motion can travel away from the moving object fast enough that no appreciable shock or bow wave can develop, and is characterized by speeds lower than about 80% the speed of sound. In the transonic regime, a bow wave forms and causes interaction with the projectile, and typically ranges from roughly 80% to 120% of the ambient speed of sound. In the supersonic regime, characterized by speeds above 120% of the ambient speed of

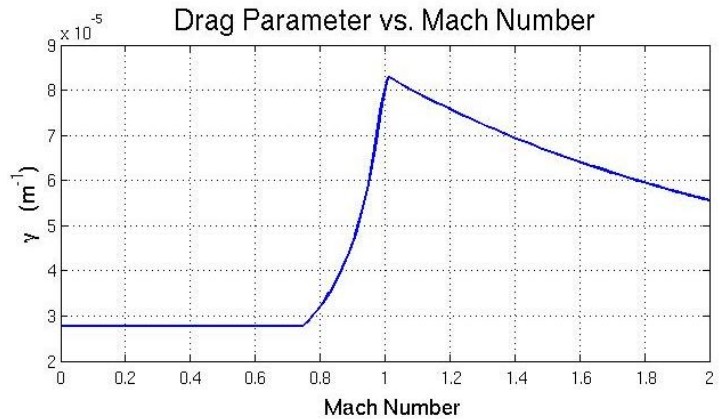


Figure 1. Model drag parameter as a function of Mach number.

of the ambient speed of sound.

sound, shock waves form around various surface features of the projectile, often dominated by the nose and base regions.

We further separate out the ballistic coefficient into two terms, x_{β_0} and $x_{\Delta\beta}$ above, the first of which is estimated in filter initialization, and the second of which is updated when new measurements are incorporated into the state estimate. These parameters are related to the ballistic coefficient through the relationship

$$\beta^{-1} = \mathbf{x}_{\beta_0}^{-1} - \mathbf{x}_{\beta_0}^{-2} \mathbf{x}_{\Delta\beta}.$$

This is essentially a change of variable that brings the Kalman filter into a more linear form.

The second type of dynamics considered here for ballistic propagation includes a constant acceleration component, x_a . This acceleration can account for the cross range motion typical of a spin stabilized projectile. The equations of motion defining this type of dynamics are given by

$$\begin{aligned} \frac{d}{dt} \mathbf{x}_p &= \mathbf{x}_v & \mathbf{x}_p(t) \Big|_{t=0} &= \mathbf{x}_{p,0}, \\ \frac{d}{dt} \mathbf{x}_v &= \mathbf{g} - \frac{\rho}{2\mathbf{x}_{\beta_0}} |\mathbf{x}_v| \mathbf{x}_v + \frac{\rho}{2\mathbf{x}_{\beta_0}^2} |\mathbf{x}_v| \mathbf{x}_v \mathbf{x}_{\Delta\beta} + \mathbf{x}_a & \mathbf{x}_v(t) \Big|_{t=0} &= \mathbf{x}_{v,0}, \\ \frac{d}{dt} \mathbf{x}_a &= 0 & \text{, with initial conditions } \mathbf{x}_a(t) \Big|_{t=0} &= \mathbf{x}_{a,0}, \\ \frac{d}{dt} \mathbf{x}_{\Delta\beta} &= 0 & \mathbf{x}_{\Delta\beta}(t) \Big|_{t=0} &= \mathbf{x}_{\Delta\beta,0}, \\ \frac{d}{dt} \mathbf{x}_{\beta_0} &= 0 & \mathbf{x}_{\beta_0}(t) \Big|_{t=0} &= \mathbf{x}_{\beta_0}. \end{aligned}$$

Other types of dynamics could be considered to achieve the objective outlined above. For instance, one natural approach is to introduce components of acceleration perpendicular to the velocity vector. Such an approach would require the addition of only two more unknown parameters for the filter estimation. However, the resulting equations of motion would be more complicated than those described above and would result in a different type of motion. The choice to use this form of dynamics in this analysis is made based on the simplicity of the filter update equations and the linear nature of the coupling of the process noise of this term with the other state variables.

An important feature of the current investigation is the nonlinear form of the aerodynamic drag as a function of velocity. We are interested in predicting the impact point of ballistic projectiles, and as such require a drag template for prediction. If the ballistic projectile is tracked through apogee before IPP estimation is required, then the up-leg track data history of $x_{\Delta\beta}$ may be suitable to predict the drag on the down-leg component of flight. However, the amount and quality of such track data is often not sufficient for this purpose, since the sensor may not have the resources or capability to dedicate track energy to all of the up-leg flight or IPP estimation may be desired when only a portion of the up-leg trajectory has been observed. In such situations, a drag template can be selected from a library of drag curves to aid in the prediction of impact point. Although the IPP errors resulting from the use of an imperfect drag template can be significant, we assume for this analysis that such a drag curve is available and do not address their creation further in this analysis.

3. KALMAN FILTER EQUATIONS

The Kalman filters used within the IMM estimator to create results for this paper extrapolate with a fourth order Runge-Kutta propagator and use the standard EKF measurement update equations. Specifically, suppose that the last time a measurement was incorporated into the filter occurred at time t_k . Define $x_{t_k}^+$ to be the state estimate after the last

measurement update, and x_t^- for $t \geq t_k$ to be the propagated state. The state estimate $x_{t_k}^+$ is a random variable, assumed to have a Gaussian distribution characterized by the state covariance matrix $P_{t_k}^+$. The state dynamics are represented by a first order system of equations in both types of filters described in the previous section, and can be written compactly using the notation

$$\frac{d}{dt} x_t^- = f(x_t^-) \quad x_0^- = x_0^+$$

The Runge-Kutta integration of this state equation, starting with initial condition $x_{t_k}^+$, is represented by $\Phi_{t-t_k} x_{t_k}^+$, so that $x_t^- = \Phi_{t-t_k} x_{t_k}^+$. It follows that the covariance of the propagated state satisfies the differential inequality

$$\frac{d}{dt} P \leq \frac{\partial f}{\partial x}(x_t^-)P + P \frac{\partial f}{\partial x}(x_t^-) + \Delta Q, \quad P_0^- = P_{t_k}^+,$$

for some process noise term ΔQ . The equation for the covariance can be solved by Runge-Kutta integration as well, although the fact that x_t^- has already been computed allows for good numerical solutions of this equation without resorting to such a method [7]. Denote the resulting integrated process noise by Q_{t-t_k} . The fundamental solution to this equation can be written in the form $P_t^- = \Psi_{t-t_k} P_0^- \Psi_{t-t_k}^T$, and the solution to the above inequality takes the form

$$P_t^- \leq \Psi_{t-t_k} P_0^- \Psi_{t-t_k}^T + Q_{t-t_k}.$$

A measurement z_{k+1} taken at time $t_{k+1} \geq t_k$ with estimated covariance R_{k+1} is incorporated in the usual manner [7]. The measurement is assumed to be Gaussian distributed with covariance R_k . In the cases considered here, the measurement is generated by a sensor model in which Gaussian noise is added to the RUV values of the true target trajectory. The state is updated from x_t^- to $x_{t_{k+1}}^+$ with the measurement using the state-to-measurement map

$h(x_{t_{k+1}}^-)$ and its derivative $H = \frac{\partial h}{\partial x}(x_{t_{k+1}}^-)$ by computing the following terms:

$$\begin{aligned} K^- &= P_{t_{k+1}}^- H_{k+1}^T (H_{k+1} P_{t_{k+1}}^- H_{k+1} + R_{k+1})^{-1} \\ x_{t_{k+1}}^+ &= x_{t_{k+1}}^- - K^- (H_{k+1} x_{t_{k+1}}^- - z_{k+1}) \\ P_{t_{k+1}}^+ &= P_{t_{k+1}}^- - K^- H_{k+1} P_{t_{k+1}}^- \end{aligned}$$

3. IMM FILTER IMPLEMENTATION

The target motion model described in Section 2 encompasses both ballistic and accelerating motion. Since the munitions under track can transition between these motion models, accurate prediction of their impact points must accommodate such shifts in the motion models. Although a number of filtering techniques [6] could be used to address this problem, the IMM estimator is chosen for its computational efficiency. Rather than using it solely to track the targets, this paper proposes using it as a filter-bank to sort through target dynamics and dynamic uncertainty, thus coarse tuning the target state representation and process noise model.

We are assuming four filter types, with each filter characterized by its use of an A-filter or B-filter model and either high or low process noise. In order to describe the filter model, we first introduce some basic notation. The process noise is set to a diagonal in all filters. The position, velocity, ballistic correction, and acceleration terms are set

independently, and are denoted as ΔQ_p , ΔQ_v , $\Delta Q_{\Delta\beta}$, and ΔQ_a respectively. Here the process noise terms are process noise rates, and so their natural units are divided by seconds. For example a position has units of meters, the position covariance has units of square meters, and the process noise rate has units of square meters per second. The process noise rate choices for the filters used in the IMM for this paper are as follows:

- Filter 1: B-filter (7 states) with diagonal process noise matrix defined by $\Delta Q_p = 0.1 \text{ m}^2/\text{s}$, $\Delta Q_v = 0.01 \text{ m}^2/\text{s}^2/\text{s}$, $\Delta Q_{\Delta\beta} = 1.0 \times 10^4 \text{ kg/m}^2/\text{s}$.
- Filter 2: B-filter, high process noise (7 states) with diagonal process noise matrix defined by $\Delta Q_p = 1 \text{ m}^2/\text{s}$, $\Delta Q_v = 0.1 \text{ m}^2/\text{s}^2/\text{s}$, $\Delta Q_{\Delta\beta} = 1.0 \times 10^6 \text{ kg/m}^2/\text{s}$.
- Filter 3: A-filter (10 states) with diagonal process noise matrix defined by $\Delta Q_p = 0.1 \text{ m}^2/\text{s}$, $\Delta Q_v = 0.01 \text{ m}^2/\text{s}^2/\text{s}$, $\Delta Q_{\Delta\beta} = 1.0 \times 10^4 \text{ kg/m}^2/\text{s}$, and $\Delta Q_a = 0.005 \text{ m}^2/\text{s}^4/\text{s}$.
- Filter 4: A-filter, high process noise (10 state) with diagonal process noise matrix defined by $\Delta Q_p = 1.0 \text{ m}^2/\text{s}$, $\Delta Q_v = 0.1 \text{ m}^2/\text{s}^2/\text{s}$, $\Delta Q_{\Delta\beta} = 1.0 \times 10^6 \text{ kg/m}^2/\text{s}$, and $\Delta Q_a = 0.05 \text{ m}^2/\text{s}^4/\text{s}$.

These filters are propagated using the dynamical process mentioned in Section 3. These states are mixed at measurement time to produce the IMM tracker. Following [6], we define our notation for the IMM process as follows:

- $\mu_{k|k}^i$ is the probability of filter i given all measurements up to time k.
- $p_{j,i}^{(k)}$ is the probability of the state dynamics being described by filter i at time k, given that the dynamics were described by filter j at time k-1.
- $X_{k|k}^i$ is the state estimate assuming filter i at time k, and given measurements through time k.
- $P_{k|k}^i$ is the covariance of $X_{k|k}^i$.
- Φ_k^j is the propagator for the jth dynamic model that propagates for time $t_{k+1} - t_k$.
- Ψ_k^j is the fundamental matrix solution of the jth dynamic model Ricatti equation for the covariance corresponding to the time interval $t_{k+1} - t_k$.
- Q_k^j is the integrated process noise for the jth dynamic model corresponding to time interval $t_{k+1} - t_k$.

This IMM estimator is broken into a five step process [6], as described below.

1. Mixing of the state estimates: For each of the model change probabilities $p_{j,i}^{(k)}$, compute

$$\begin{aligned} \mu_{k-1|k-1}^{ji} &= \sum_{j=1}^4 \mu_{k-1|k-1}^j \mathbf{1}_{k-1|k-1}^i - p_{j,i}^{(k)} \\ Y_{k-1|k-1}^i &= \sum_{j=1}^4 X_{k-1|k-1}^j \mu_{k-1|k-1}^{ji} \\ P_{k-1|k-1}^{Y,i} &= \sum_{j=1}^4 \mu_{k-1|k-1}^{ji} \mathbf{1}_{k-1|k-1}^j + \mathbf{1}_{k-1|k-1}^j - Y_{k-1|k-1}^j \mathbf{1}_{k-1|k-1}^j - Y_{k-1|k-1}^j \end{aligned}$$

2. Model conditioned updates: Compute the new state and covariance estimates using the new measurement.

$$\begin{aligned}
X_{k|k-1}^i &= \Phi_k^i(Y_{k-1|k-1}^i) \\
P_{k|k-1}^i &= \Psi_k^i P_{k-1|k-1}^{Y,i} \Psi_k^{i^T} + Q_k^i \\
S_k^i &= H_k^i P_{k|k-1}^i H_k^{i^T} + R_k \\
K_k^i &= P_{k|k-1}^i H_k^{i^T} \mathbf{I}_k^{-1} \\
\tilde{Z}_k^i &= Z_k^i - H_k^i X_{k|k-1}^i \\
X_{k|k}^i &= X_{k|k-1}^i + K_k^i \tilde{Z}_k^i \\
P_{k|k}^i &= P_{k|k-1}^i - K_k^i H_k^i P_{k|k-1}^i
\end{aligned}$$

3. Model likelihood computations: Compute the likelihood of the model i at time k given the filter residuals \tilde{Z}_k^i .

$$\Lambda_k^i = \det \left(\frac{1}{S_k^i} \right) \exp \left(-\frac{1}{2} \tilde{Z}_k^{i^T} \mathbf{I}_k^{-1} \tilde{Z}_k^i \right)$$

4. Update of model probabilities:

$$\mu_k^i = \left(\sum_{j=1}^4 \Lambda_k^j \mu_{k|k-1}^j \right)^{-1} \Lambda_k^i \mu_{k|k-1}^i$$

Combination of state estimates: The state estimates are blended for use in IPP. Three methods are considered for this step, as described in the next section.

4. IMM BLENDING FOR IPP

Three approaches are considered for blending the results for IPP using IMM filters with and without mixing. The first approach propagates the filter with the highest mode probability to the ground, and uses the filter covariance projected onto the ground to estimate the ground plane covariance. The second method propagates all model outputs to the ground, where it blends their IPPs using the mode probabilities associated with each track. The third method first blends the tracks at the time of the last measurement and propagates this track to the ground, again estimating the ground plane covariance using the projection of the propagated covariance into the ground plane. These three blending methods are described algorithmically as follows:

- Blending Method 1 (BM1): Propagate using filter with highest mode probability

1. Compute IPP time $t_{k|k}^{IPP}$ from $X_{k|k}^{j \max}$ using $\Phi_{t_{k|k}}^{j \max} X_{k|k}^{j \max}$, where $j \max$ is the filter with the highest mode probability μ_k^j .

2. Compute the impact point and covariance using a ballistic template to deal with drag variable Mach.

$$\begin{aligned}
X_{k|k}^{IP,j \max} &= \Phi_{t_{k|k}}^{j \max} X_{k|k}^{j \max} \\
P_{k|k}^{IP,j \max} &= \Psi_{t_{k|k}}^{j \max} P_{k|k}^{j \max} \Psi_{t_{k|k}}^{j \max^T}
\end{aligned}$$

3. Project the j state estimate and covariance onto the ground using the state space to ground plane projections

$$\Pi_{n_j \rightarrow 2}$$

$$X_{k|k}^{2dIP} = \prod_{n \rightarrow 2}^{j \max} X_{k|k}^{IP, j \max}$$

$$P_{k|k}^{2dIP} = \prod_{n \rightarrow 2}^{j \max} \Psi_{t_{k|k}^{IPP, j}}^{j \max} P_{k|k}^{j \max} \Psi_{t_{k|k}^{IPP, j}}^{j \max T} \prod_{n \rightarrow 2}^{j \max T}$$

- Blending Method 2 (BM2): Propagate and blend.

1. For each IMM model, compute IPP time $t_{k|k}^{IPP, j}$ from $X_{k|k}^j$ using $\Phi_t^j(X_{k|k}^j)$

2. Compute the impact point and covariance using a ballistic template to deal with drag variable Mach.

$$X_{k|k}^{IP, j} = \Phi_{t_{k|k}^{IPP, j}}^j(X_{k|k}^j)$$

$$P_{k|k}^{IP, j} = \Psi_{t_{k|k}^{IPP, j}}^j P_{k|k} \Psi_{t_{k|k}^{IPP, j}}^{j T}$$

3. Project the j state estimate and covariance onto the ground using the state space to ground plane projections

$$\Pi_{n_j \rightarrow 2}$$

$$X_{k|k}^{2dIP, j} = \prod_{n \rightarrow 2}^j X_{k|k}^{IP, j}$$

$$P_{k|k}^{2dIP, j} = \prod_{n \rightarrow 2}^j \Psi_{t_{k|k}^{IPP, j}}^j P_{k|k} \Psi_{t_{k|k}^{IPP, j}}^{j T} \prod_{n \rightarrow 2}^{j T}$$

4. Compute the blended state and covariance in the two dimensional ground plane.

$$X_{k|k}^{2dIP} = \sum_{j=1}^4 X_{k|k}^{2dIP, j} \mu_k^j$$

$$P_{k|k}^{2dIP} = \sum_{j=1}^4 \mu_k^{2dIP, j} \left[P_{k|k}^{2dIP, j} + X_{k|k}^{2dIP, j} X_{k|k}^{2dIP, j} - X_{k|k}^{2dIP} X_{k|k}^{2dIP, j} - X_{k|k}^{2dIP, j} X_{k|k}^{2dIP T} \right]$$

- Blending Method 3 (BM3): Blend and propagate.

1. Compute the blended state and covariance

$$X_{k|k} = \sum_{j=1}^4 X_{k|k}^i \mu_k^i$$

$$P_{k|k} = \sum_{j=1}^4 \mu_k^i \left[P_{k|k}^i + X_{k|k}^i X_{k|k}^i - X_{k|k} X_{k|k}^i - X_{k|k}^i X_{k|k}^T \right]$$

2. Compute IPP time, $t_{k|k}^{IPP}$, from $X_{k|k}$ using $\Phi_t^{j \max}(X_{k|k}^{j \max})$, where j_{\max} is the filter with the highest mode probability μ_k^j .

3. Compute the impact point and covariance using a ballistic template to deal with drag variable Mach. This function has to be pulled from a template on the up-leg for unobserved velocities, but filter estimates are used for observed Mach regions. By apogee, all relevant Mach values have been observed.

$$X_{k|k}^{IP} = \Phi_t^{j \max}(X_{k|k}^{j \max})$$

$$P_{k|k}^{IP} = \Psi_{t_{k|k}^{IPP}}^{j \max} P_{k|k} \Psi_{t_{k|k}^{IPP}}^{j \max T}$$

4. Project the 7 or 10 state estimate and covariance onto the ground [7], to obtain ground plane IP and IPP error estimate.

5. RESULTS

The IMM investigation for IPP includes variation across targets (2), target Mach number (3), IMM mixing methods (2), and IMM blending methods (3), for a total of 36 conditions. The focus of this paper is on blending methods for IPP with consideration of Mach characteristics. We will simply note here that differences between the results using the two target types and two mixing methods were not significant, and the specific results we present for the 10 state projectile using both mixing and blending are representative of the general behavior observed across the other target types and mixing methods.

Analysis runs consist of 20 Monte Carlo trials with noise drawn from Gaussian distribution with a standard deviation in position of 50 m at 20 km. The results of the IMM blending approaches are separated out by the characteristic Mach region. For each of these regions, the IPP error was computed for each trajectory, and the empirical covariance in the ground plane was computed from each shot grouping for each filter. The IPP error vs. time for each of three blending methods is shown in Figure 2. IPP Errors for the three blending methods are shown for the subsonic trajectory in (a), the transonic trajectory in (b), and the supersonic trajectory in (c). It was found that BM3, where all tracks are blended at the measurement time, outperformed the other two blending methods in all three Mach regions, and for both target types. It was particularly interesting to note that BM1, which performs IPP using the filter with the highest mode probability, underperformed ground blending as implemented in BM2.

The empirical standard deviation for the various blending methods is shown in Figure 2.(d), (e) & (f). For an empirical covariance matrix \mathbf{P} , the metric used is the square root of the sum of the eigenvalues of \mathbf{P} . This serves as a characteristic distance associated with the spread of impact points around the empirical mean. Notice that the covariance terms are not as large as the observed IPP error due to a biasing of the IPP.

6. CONCLUSIONS

The use of the IMM for prediction of IPP and IPP covariance was considered in this paper. The following three methods were considered: BM1, propagation of the track estimate with the highest IMM mode probability; BM2, propagation of each of the tracks independently to the ground followed by a blending step that used the track mode probabilities; and BM3, blending of the track after the most recent measurement followed by propagation to the ground using the highest mode probability propagation model. It was found that BM3 exhibited the best performance across each of the 6 target models considered, regardless of whether mixing was used in the track update step or not.

7. REFERENCES

1. H.A.P. Blom, and Y. Bar-Shalom, "The Interacting Multiple Model Algorithm for Systems with Markovian Switching Coefficients," IEEE Trans. Auto. Cont., 1988, pp. 780-783.
2. Bar-Shalom, Y.,
3. Bar-Shalom, Y., Blair, W.D., editors, "Multitarget-Multisensor Tracking: Applications and Advances Volume III," Artech House, Norwood, MA, 2000, pp. 499-561.
4. Mazor, E., Averbuch, A., Bar-Shalom, Y., and Dayan, J., "Interacting Multiple Model Methods in Target Tracking: A Survey," IEEE Transactions on Aerospace and Electronic Systems, Jan. 1998, pp. 103-123.
5. McCoy, Robert L., "Modern Exterior Ballistics: The Launch and Flight Dynamics of Symmetric Projectiles," Schiffer Publishing Ltd., 1999
6. Blair, W.D., "Derivation of the Interacting Multiple Model Algorithm for Systems with Markovian Switching Coefficients," preprint.
7. Kerce, J. Clayton, Brown, George C., "A Flow Field Approach for State Dynamics in Statistical Filtering," in preparation.

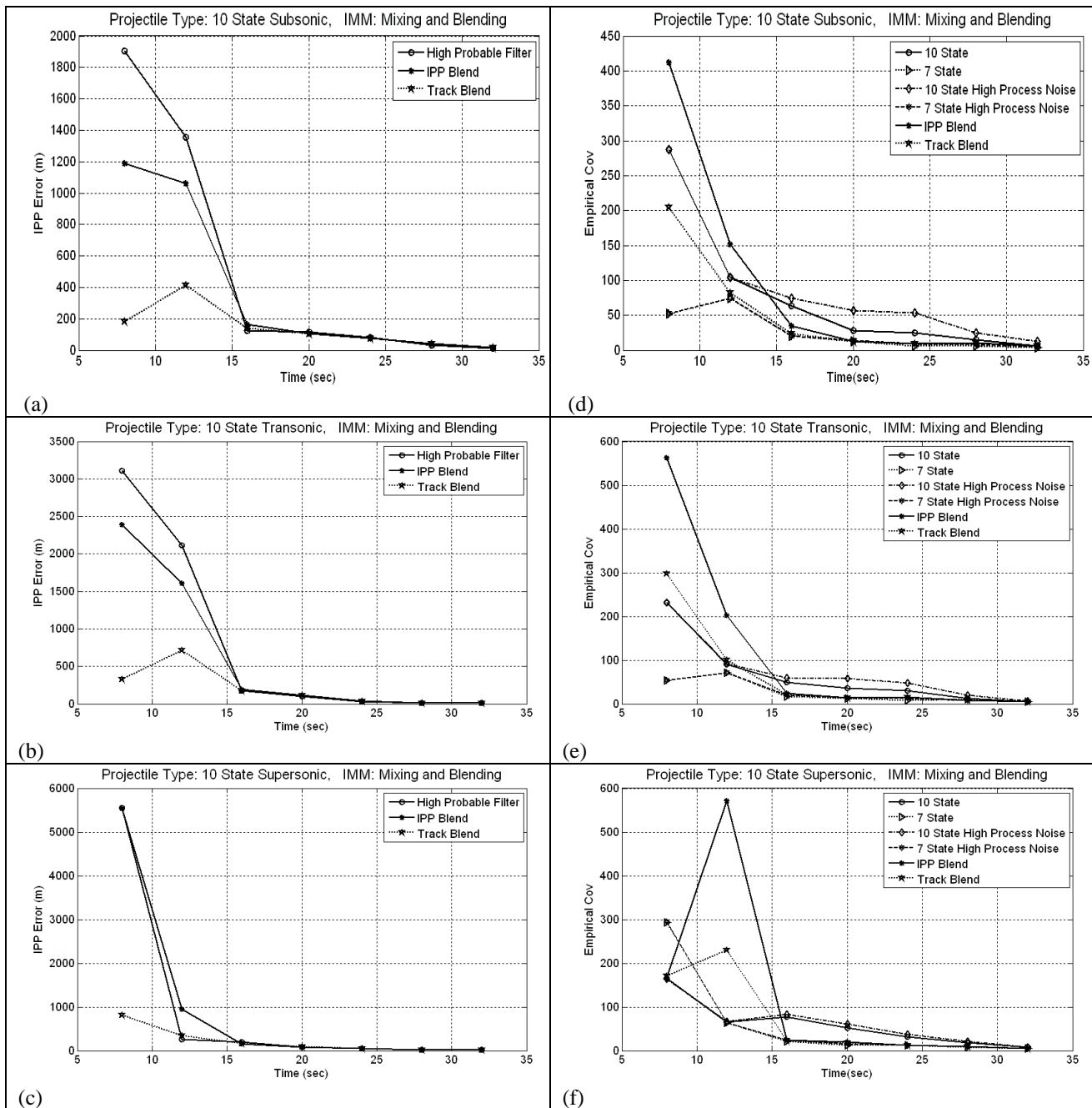


Figure 2 Empirical IPP errors for 10 state trajectory characterized by subsonic (a), transonic (b), and supersonic (c) Mach number. Empirical covariances for these same cases are shown in (d),(e), and (f).